Jour. of the KGS, Vol. 20, No. 7. September 2004, pp. 45~55

Size Effect of Specimen and Aggregate on Fracture Characteristics of Cemented Sand

경화 모래의 파괴 특성에 대한 시료 및 입자의 크기 영향

Kim, Tae-Hoon[1] 김 태 훈
Lee, Kang-Il[2] 이 강 일
Im, Eun-Sang[3] 임 은 상

요 지

경화 모래와 같은 단단한 흙에서는 자주 파괴시의 응력이 실내실험을 통해 얻은 전단강도 보다 작을 뿐만 아니라 일반적인 해석방법이 적절하지 못한 경우를 보게된다. 여러 학자들은 이러한 현상이 일어나는 것은 흙속에 있는 균열이나 절리와 같은 불연속이 존재 하기 때문일거라 생각했고, 따라서 파괴역학이 이런 흙에대해서는 더 적절한 해석방법이 될 수도 있다고 생각 해왔다. 그러나 파괴역학의 개념을 도입하기에는 파괴 요소들이 재료의 구성뿐만 아니라 시료 그리고 입자의 크기에 크게 영향을 받기 때문에 어려움이 많이 있다. 본 연구에서는 경화모래의 파괴 특성에 시료와 입자의 크기가 미치는 영향을 기술한다. 실내실험 결과, 시료와 입자의 크기는 경화모래의 파괴 거동에 많은 영향을 미치는 것을 보여준다.

Abstract

In the past it has been often observed that the shear stresses at failure are much smaller than the shear strength obtained from traditional laboratory tests and conventional analysis technique is inadequate in stiff soil, such as cemented sand. Many researchers have brought attention to the fact that the presence of flaws i.e. fissures, cracks, joints have a great effect on the strength and overall stress-strain behavior of such materials. They have thought that fracture mechanics may appropriately be adopted as a good tool for analysis of these materials. However, the use of fracture mechanics concept especially for cemented sands is faced with difficulties in obtaining relevant parameters, because fracture parameters and predictions are highly dependent on the material constituents and the size of specimens as well as the size of particles. This paper addresses the effects of sizes which include specimen and aggregate on fracture properties of cemented sand. The results of laboratory tests show that the sizes of specimens and particle have a great effect on the fracture properties such as nominal strength of cemented sand.

Keywords : Cemented sand, Crack, Fracture mechanics, Nominal strength, Shear strength, Size effect

1. Introduction

For a couple of decade, many engineers have often observed that the shear stresses at failure are much smaller than the shear strength obtained from traditional laboratory tests, basic limiting equilibrium analysis, and

1 Member, Ph.D, Associate Researcher, DAEWOO E&C (tkim@dwconst.co.kr)
2 Member, Associate Prof., Dept. of Civil Engrg., Daejin Univ.
3 Member, Ph.D, Researcher, Korea Water Resources Corporation

the failure mechanism is often different when they encountered design and analysis challenges involving natural and man-made slopes, shallow and deep foundations, and deep excavations in stiff or brittle soils. In the past it was often unclear what caused the reduction of the overall strength, and what led to a different failure mode. It is generally known that presence of discontinuities, such as cracks, fissures and joints in soil mass have a great effect on the strength and the behavior of solid and especially brittle materials. That is, any flaw such as cracks, fissures, and joints induce or cause stress concentrations, so that local failure might occur and finally lead to a reduction in the overall strength of the material and the earth structure systems. In most cases, nevertheless, the soil has been treated as a continuous and homogeneous material, and failure criteria ranging from traditional strength of materials approaches, such as the Mohr-Coulomb criterion, to more complex constitutive formulations have been widely used. However, these criteria may not be applicable to all kinds of soils. For all cohesionless granular and normally consolidated soils the classical strength is quite satisfactory. However, for brittle and cohesive materials, especially for fissured over-consolidated clays and cemented sands, which are characterized by a nominal peak shear strength followed by a residual shear strength, it seems not to be applicable (Rizkallah, 1977). Very recently, LEFM (Linear Elastic Fracture Mechanics) has been applied to geotechnical engineering problems. Unlike any other cementitious materials, such as concrete, cemented sands have a different bonding structure. There are usually two bonding structures, which include void bonding and contact bonding. Especially for contact bonding, cementing agents surrounding particles make them adhere to each other. That is, the finer the particle is, the closer it is to void bonding. It means that cementation depends on the size of the particles. So, if cementation is dependent on the size of the particles, so will the behavior of the cemented sand. In addition, the fracture behavior is different with respect to the size of geometry despite the same particle size. This means that the fracture parameters are highly dependent on the size of the geometry and aggregate. The use of fracture mechanics concepts in cemented soils, therefore, is closely connected to our understanding of size effect issues. In this study, an experimental program to investigate the size effects that include the geometry of a specimen configuration and the size of grains in cemented sand was designed. To achieve this, different specimen dimensions with different sizes of grains were used.

2. Experiment

2.1 Four Point Test

A short beam specimen that is subjected to four-point bending was first developed by Iosipescu (1967), and it has since received great attention in the fracture mechanics community. The shear and bending moment diagrams along the specimen are shown in Fig. 1. Although the four-point beam specimen also usually fail to develop pure a Mode II conditions which is sliding mode, the technique is still widely used due to the following salient features related to this test.

- The geometry provides nearly constant shear and almost zero moment in the main section of interest

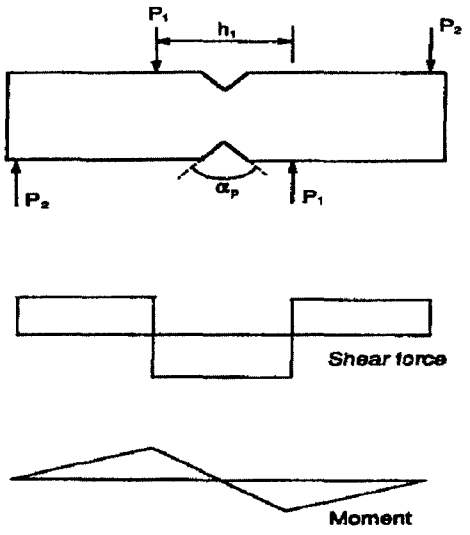

Fig. 1. The shear and bending moment diagrams along the four point beam specimen proposed by Iosipescu (Shah et al., 1995)

as shown Fig. 1.

- The test section is doubly notched.
- The test fixture is designed to prevent rotation of the test specimen.
- Post-peak behavior can be monitored using Crack Mouth Sliding Displacement (CMSD).

In view of the above advantages, the four-point bending specimen and loading configuration were adopted in this study.

2.2 Material

Three different sands with different grain size distributions were used in the experimental program, which include fine, intermediate and coarse gradations. Grain size distributions for the three sands, which are quartz Ottawa sands, are shown in Fig. 2. As we can see, they are all classified as poorly graded sands (SP), and the maximum particle sizes are about 0.31 mm, 1.1 mm, and 1.9 mm respectively.

The specific gravity, unit dry weight ranges, and maximum and minimum void ratios are given in Table 1.

Table 1. Properties of three different quartz sands

	Gs	γ_d (kn/m^3)	e_{max}	e_{min}
Fine	2.65	16.59~17.11	0.805	0.486
Intermediate	2.64	14.93~15.48	0.927	0.667
Coarse	2.63	14.93~14.99	1.06	0.721

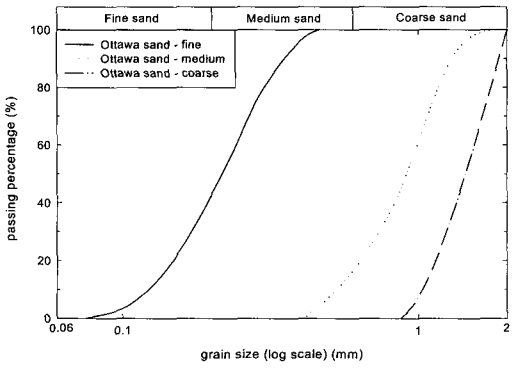

Fig. 2. Grain size distribution curves for three quartz sands

2.3 Cementing Agent and Specimen

It is in general not easy to obtain samples from the field due to the following difficulties: (a) The soil could easily become decemented or fail during sampling, and (b) the soil may have different cementing agents and amounts at different locations, which would lead to specimen non uniformities. In view of the above considerations, using naturally cemented samples may cause significant scatter in the experimental results with wide ranges of properties. Artificially cemented specimens were therefore used instead. The main advantages of using artificially cemented specimens are: (a) ability to obtain uniform specimens, and, (b) ability to control variables such as grain size and the amount of cementation. Different cementing agents have been used in the past to make specimens e.g. Portland cement, wax, etc. However, it is often difficult to ensure uniformity of the cementing agent within several specimens. After several trials, we decided to use ordinary household sugar dissolved in warm tap water, which was diffused into the initially cohesionless sand specimen, which was subsequently left to dry. This technique has successfully been used as a cementing agent I in the past (Mould, 1983). This agent was also selected by Alqasabi (1998), because it was easy to obtain and handle, especially in terms of manufacturing the specimens. Hence, it was used again in this research. Since the main objects of this study are to investigate mixed mode-fracture-related behavior of cemented sand, several factors must be taken into account.

- All specimens should be geometrically similar
- The specimens should be large enough and have configurations so that plane strain conditions can be accurately simulated during testing

The considerations can be satisfied by setting the same aspect ratio such as constant depth-to-length ratio. According to American Society of Testing and Material (ASTM Designation E399-74) the ratio of the depth to length should be 1:4 to ensure a plane strain condition.

Table 2. Specimen dimensions

	Length (mm)	Depth(mm)	Width(mm)
Small	203.2	50.8	101.6
Intermediate	406.4	101.6	101.6
Large	812.8	203.2	101.6

We therefore have adopted this ratio for the entire experimental program. While the depth and length are varied with this ratio, the width of a specimen is fixed. According to ASTM, the dimension of the standard specimens for plane strain condition should be such that the depth D is twice the width W, or if this leads to impractical specimen dimensions, ASTM suggests that the width W might be between 0.25D and D. Based on this reference, the final dimensions of three specimens are given in Table 2. To make the specimens, different sizes of rectangular molds made of Lucite were used. The molds consist of several parts that are fastened with screws.

2.4 Procedure for Specimen Preparation

Once the parts of the mold were put together the mold was filled with dry sand. To make specimens with uniform density a raining technique was used. After raining, the excess sand was removed and the sand was leveled at the top of the mold. The mold with dry sand was then carefully weighted. In the meantime a sugar-water mixture with 25% by weight of sugar was prepared in a separate large container. Regular hot tap water was used, and the mixture was stirred until the sugar was completely dissolved in the water. The prepared mold with dry sand was carefully immersed in the sugar-water mixture and left for about 24 hours to allow for all entrapped air in the sand to escape. After being fully saturated the mold was removed from the mixture tank, and weighed. Again, the mold containing the wet sand specimen was left to drain for several days, because the specimen was very weak and sensitive to disturbance immediately after removal from the container, so it was not able to stand by itself. Once the specimen had reached a certain level of dryness the Lucite mold was then carefully disassembled. The moist cemented sand specimen was thereafter left to air dry completely at room temperature. All the specimens were prepared in this manner. After the specimens were completely dried, a pair of symmetric notches, whose depths were one-sixth of the depth of the specimens, were cut in the middle section of each specimen using a thin hacksaw blade.

3. Test

All specimens were tested in a MTS servo-controlled hydraulic load frame. The shear force was produced by the four point loading arrangement as shown in Fig. 3. The loading positions were always kept as d/12 from the notches and the edge of the specimen. Once the specimen was mounted in the experimental apparatus, a clip gauge consisting of a full bridge circuit with four strain gauges mounted on two cantilever beams was set up at the mouth of the upper notch to measure CMSD (Crack Mouth Sliding Displacement). The specimens were tested at a constant displacement rate. Although, at the beginning of the tests, we assumed that the fracture parameters and the behavior of the brittle cemented sandy material would be independent on the loading rate, we set the loading rate at 0.05 mm/min (0.002 in/min), because for soft synthetic rock-like materials that do not display viscous effects, according to Harberfield and Johnson (1989), fracture toughness measurements would not be affected by a change in the loading rate, if it is less than 0.1 mm/min (0.004 in/min). During testing, all data such as load and CMSD were transmitted to the computer recording system through the DAS (Data Acquisition System) and monitored using LabView

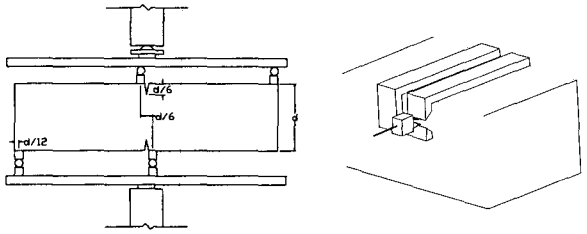

(a) overall view (b)clip gauge

Fig. 3. Geometry of test specimen and load arrangement

computer software simultaneously. Loading was applied to the specimen until the crack began to propagate. Initially, before the crack began to propagate, the CMSD increased almost linearly with respect to the applied load. However, once the crack started to significantly propagate the relation between the applied load and the CMSD changed in a nonlinear manner. That is, values of the CMSD would increase much faster. At that stage, the loading was reversed. Cycles of loading-unloading were generated frequently during testing, and all tests were carried out with this closed-loop CMSD monitoring taking place.

4. Discussion

Several specimens were fabricated for studying fracture behavior of cemented sand. It was very difficult to make specimens with increasing particle sizes because of handling sensitivity. Fig. 4 through Fig. 8 show the relationships between applied load and CMSD. In the case of the fine sand, the initial slopes of the load-displacement response are almost the same for each size. The CMSD corresponding to the peak load for small and larger size specimens were about 0.098 mm and 0.19 mm respectively. For most of the cases, except for the intermediate size and large specimens of fine sand, no crack initiation and propagation was observed before failure. It means that the load increased almost linearly until reaching the peak load level, and failure occurred suddenly after the peak load was reached. Clearly, this configuration was very brittle. Since the load-displacement response curve before the peak point was

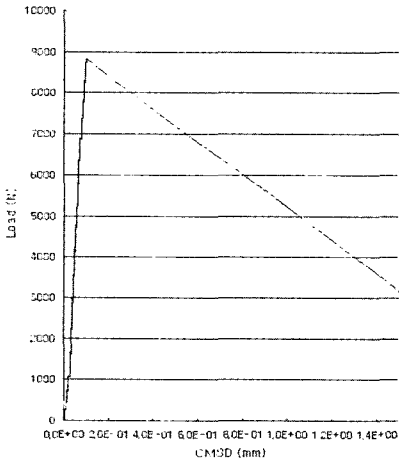

Fig. 4. Load vs CMSD for small fracture specimen (F-S-1)

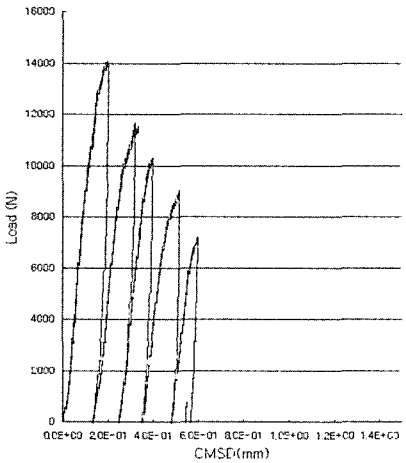

Fig. 6. Load vs CMSD for large fracture specimen (F-L-1)

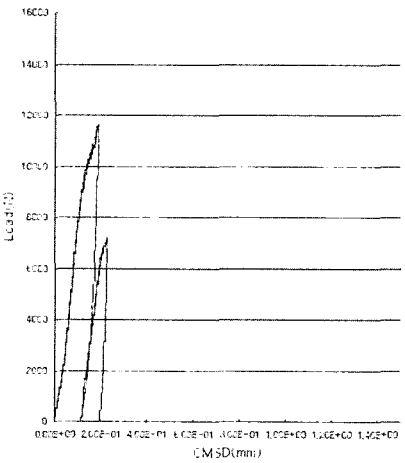

Fig. 5. Load vs CMSD for medium fracture specimen (F-M-5)

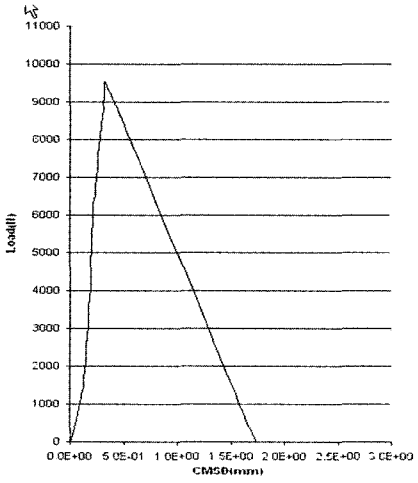

Fig. 7. Load vs CMSD for small fracture specimen (I-S-3)

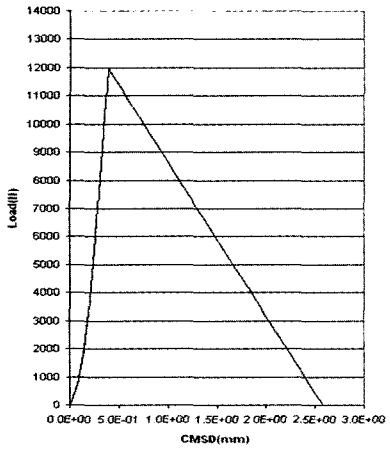

Fig. 8. Load vs CMSD for intermediate fracture specimen (I-M-1)

almost straight, it was very difficult to find or detect the point, where unloading should take place. However, as the size of the specimen increased, crack initiation and some minor degree of propagation were observed before complete failure occurred. Cracks initiated at the tip of the notch, and propagated not straight down, but rather sideway as shown in Fig. 9. That means that the cracks always seemed to propagate in the direction that is normal to the maximum principal stresses. Similar to the results observed by Alqasabi (1998), the intermediate and larger samples of fine sand had measurable values of permanent CMSD in each load-unload cycle. This might be due to the effect of the fracture process zone which causes permanent displacements. The summary of the test results is presented in Table 3, which shows the dimensions and peak loads corresponding to each specimen. According to this table, the nominal peak stress decreases

Table 3 Dimension, and Peak load of Samples

Name of sample	Length (mm)	thickness (mm)	Depth (mm)	Max.Load (N)	Strength (Mpa)
F-S-1	203.20	101.2	50.80	8830.07	2.36
F-S-2	203.20	98.43	50.80	8020.46	2.15
F-S-3	203.20	101.6	50.80	7264.23	1.95
F-S-4	203.20	99.78	50.80	9194.83	2.46
F-M-1	406.40	98.43	101.60	10551.60	1.41
F-M-2	406.40	98.43	101.60	13122.78	1.76
F-M-3	406.40	96.77	101.60	13345.20	1.79
F-M-4	406.40	98.43	101.60	7117.44	0.95
F-M-5	406.40	97.43	101.60	11663.47	1.56
F-L-1	812.80	93.98	203.20	14564.06	0.98
F-L-2	812.80	94.49	203.20	14065.06	0.94
F-L-3	812.80	94.87	203.20	15966.06	1.07
I-S-1	204.70	97.03	50.80	7254.37	1.94
I-S-3	203.20	97.79	50.80	9513.22	2.55
I-S-4	203.20	101.60	50.80	9448.06	2.53
I-S-5	203.20	97.03	50.80	7490.61	2.01
I-S-6	203.20	101.60	50.80	8532.02	2.29
I-M-1	406.40	96.52	104.10	12010.98	1.57
I-M-2	406.40	96.52	104.60	10231.32	1.33
I-M-3	406.40	96.52	104.60	11620.03	1.51
I-M-4	406.40	96.52	106.60	8861.21	1.13
I-L-1	406.40	96.52	106.60	12062.38	0.81
C-S-1	406.40	98.43	52.38	6950.3	1.86
C-S-2	406.40	98.43	50.80	5212.72	1.40
C-S-3	406.40	96.77	50.80	5386.48	1.44
C-S-4	406.40	98.43	51.44	6646.22	1.78
C-S-5	406.40	98.43	52.38	7058.9	1.89

Where, F,I,C = sizes of grains S,M,L = Sizes of Specimens

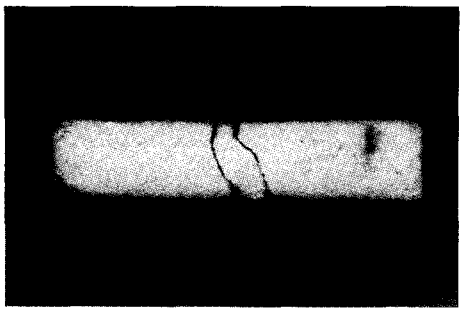

Fig. 9. Crack Propagation (I-S-1)

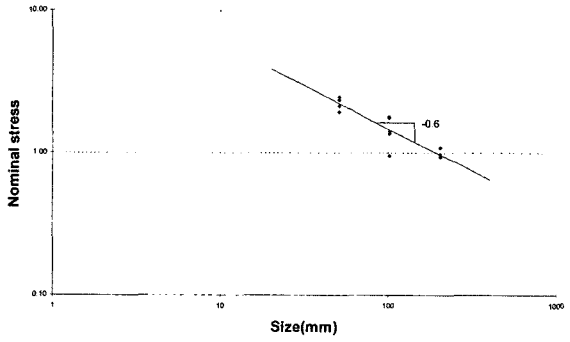

Fig. 10. Effect of Size of Geometry (Fine Sand)

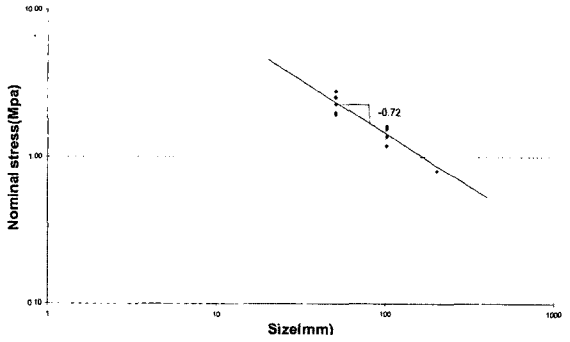

Fig. 11. Effect of Size of Geometry (Intermediate Sand)

as the geometric size increases. That is there might be a distinct size effect. The changes in nominal stress with respect to the geometry size displayed in log-log scale are shown in Fig. 10 and Fig. 11. Both diagrams present a distinct size effect. That is, the nominal peak stress decreases as the geometric size increases. However, the rate of decrease of nominal peak stress in cemented coarse sands is much steeper than that observed in cemented fine sands. It might be related to the bonding structure of the cemented sands. As we know, cemented sands have two types of bonding structures, which include the void bond and contact bond. The fine sand appears to be close to the void bond configuration, and it is far more stable. In contrast, coarse sand usually displays contact bond behavior, which fails quickly. In addition, since the fine sand has smaller voids than the coarse sand, the effect of the fracture process zone that causes the gradual decrease of the strength might be larger.

5. Size Effect Model

5.1 LEFM Approach

Consider a center crack panel with a short crack. The expression for the stress intensity factor can be written as follows

$$K_I = \sigma_N \sqrt{D} \sqrt{\pi \alpha} \tag{1}$$

Where, α = a/D, and D = a characteristic dimension

In LEFM, failure occurs when K_I reaches K_{IC}, which is a material property. Hence, at failure, from Eq (1)

$$\sigma_{NC} = \frac{K_{IC}}{\sqrt{D}\sqrt{\pi \alpha}} \tag{2}$$

Again, for the similar structures with a_k = ka the critical stress that produces crack growth is

$$\sigma_{NC}^{k} = \frac{K_{IC}}{\sqrt{D}\sqrt{\pi \alpha_k}} \tag{3}$$

Eq (3) can be rewritten as

$$\begin{aligned} \sigma_{NC}^{k} &= \frac{K_{IC}}{\sqrt{D}\sqrt{\pi k \alpha}} \\ &= \frac{1}{\sqrt{k}} \frac{K_{IC}}{\sqrt{D}\sqrt{\pi \alpha}} \\ &= \frac{1}{\sqrt{k}} \sigma_{NC} \end{aligned} \tag{4}$$

Let us assume σ_{NC} which is our reference specimens to be equal to $\sigma_{NC} = \lambda f_t$

Then Eq (4) becomes

$$\frac{\sigma_{NC}^{k}}{f_t} = \frac{\lambda}{\sqrt{k}} \tag{5}$$

By taking the logarithm

$$\log\left(\frac{\sigma_{NC}^{k}}{f_t}\right)=\log\lambda-\frac{1}{2}\sqrt{k} \tag{6}$$

The above equation indicates that the strength predicted by LEFM is reduced with size by a factor of ½ in the log-log scale.

5.2 Fracture Mechanics Approach with Permanent CMOD Offset

Alqasabi (1998) observed that LEFM was not successful in predicting the post-peak behavior for cemented sand, and that there were always certain permanent offsets in CMOD values in each load-unload cycles in the tests. Based on this observation he proposed a new size effect formulation. First, the value of CMOD at the peak load, $CMOD_{cr}$ can be divided into elastic and inelastic components as

$$CMOD_{cr}=CMOD_e+CMOD_p \tag{7}$$

where,

$CMOD_{cr}$ = Total crack mouth opening displacement

$CMOD_e$ = Elastic crack mouth opening displacement predicted by LEFM

$CMOD_p$ = permanent crack mouth opening displacement

Also, he found that there was a linear relationship between the load and the permanent CMOD offset shown in Eq (8)

$$CMOD_p=C_1\sigma_{cr}+C_2 \tag{8}$$

where, C_1 and C_2 are constant. And

$$CMOD_e=\frac{4\sigma_{cr}a}{E}g_2\left(\frac{a}{b}\right) \tag{9}$$

By substituting Eq (8) and Eq (9) into Eq (7) we get

$$CMOD_{cr}=\sigma_{cr}\left[\frac{4a}{E}g_2\left(\frac{a}{b}\right)+C_1\right]+C_2 \tag{10}$$

Again, for similar geometries in which a = ka, and b = kb Eq (10) becomes

$$CMOD_{cr}^{k}=\sigma_{cr}^{k}\left[k\frac{4a}{E}\left(\frac{a}{b}\right)+C_1\right]+C_2 \tag{11}$$

Knowing that at failure $CMOD_{cr}^{k}=CMOD_{cr}$ we obtain

$$\sigma_{cr}^{k}=\sigma_{cr}\left[\frac{\frac{4a}{E}g_2\left(\frac{a}{b}\right)+C_1}{k\frac{4a}{E}g_2\left(\frac{a}{b}\right)+C_1}\right] \tag{12}$$

Again, we assume $\sigma_{cr}=\lambda f_t$, and obtain

$$\frac{\sigma_{cr}^{k}}{f_t}=\lambda\left(\frac{1+C_2}{k+C_2}\right) \tag{13}$$

where, $C_2 = C_1/((4a/E)g_2(a/b))$

By taking the logarithm on both sides of Eq. (13) we obtain

$$\log\left(\frac{\sigma_{cr}}{f_t}\right)=\log\lambda+\log(1+C_2)-\log(k+C_2) \tag{14}$$

5.3 Size Effect Model by Bazant

Bazant (1984) has formulated a new size effect law based on the concept of an effective-elastic crack. They considered a series of geometrically similar structures, which may have different sizes, but which have a constant ratio of initial crack length a_o to characteristic dimension, D_0. Based on LEFM, the nominal strength of a structure, σ_{NC}, can be expressed as

$$\sigma_{NC}=\frac{K_{IC}}{g_1\left(\frac{a_c}{D}\right)\sqrt{\pi a_c}}=\frac{K_{IC}}{g_1\left(\frac{a_c}{D}\right)\sqrt{\Delta a_c\left(1+\frac{a_0}{\Delta a_c}\right)\pi}} \tag{15}$$

where,

K_{IC} = the critical stress intensity factor

a_c = The critical crack length

a_0 = The initial crack length

Da_c = The critical crack extension

The geometric function $g_1(a_c/D)$ can be expanded into a Taylor series as shown below.

$$g_1\left(\frac{a_c}{D}\right) \cong g_1\left(\frac{a_0}{D}\right) + g_1'\left(\frac{a_0}{D}\right)\left(\frac{a_f}{D} - \frac{a_0}{D}\right)$$
$$\cong g_1\left(\frac{a_0}{D}\right) + g_1'\left(\frac{a_0}{D}\right)\frac{\Delta a_c}{D} \quad (16)$$

Substituting Eq (16) into Eq (15) results in

$$\sigma_{NC} = \frac{K_{IC}}{\left\{g_1\left(\frac{a_0}{D}\right) + g_1'\left(\frac{a_0}{D}\right)\frac{\Delta a_c}{D}\right\}\sqrt{\Delta a_c\left(1+\frac{a_0}{\Delta a_c}\right)\pi}}$$
$$= \frac{K_{IC}}{\left\{g_1\left(\frac{a_0}{D}\right) + g_1'\left(\frac{a_0}{D}\right)\frac{\Delta a_c}{D}\right\}\sqrt{\pi\Delta a_c}\sqrt{\left(1+\frac{a_0}{\Delta a_c}\right)}} \quad (17)$$

Bazant assumed that the fracture energy dissipates at failure and is a smooth function of structural dimensions and the size of the fracture process zone. From this assumption and by introducing the following notation as

$$Bf_t = \frac{K_{IC}}{\left\{g_1\left(\frac{a_0}{D}\right) + g_1'\left(\frac{a_0}{D}\right)\frac{\Delta a_c}{D}\right\}\sqrt{\pi\Delta a_c}}$$

and

$$D_0 = \frac{D\Delta a_c}{a_0}$$

Equation (17) can be rewritten as

$$\sigma_{NC} = \frac{Bf_t}{\sqrt{1+\frac{D}{D_0}}} \quad (18)$$

Fig. 12 illustrates the size effect on the nominal strength. It is clear that the size effect model by Bazant

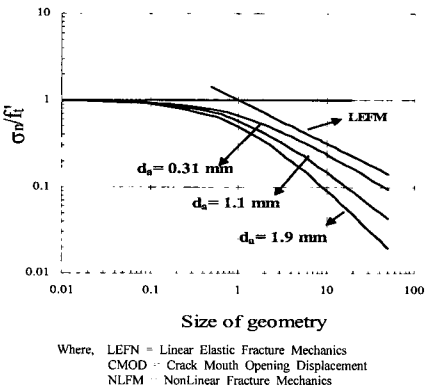

Fig. 12. Size effect on nominal failure stress

is close to a strength criterion for relatively small size specimens. On the other hand, it predicts similar nominal strength as LEFM for relatively large size specimens or structures.

5.4 Modified Bazant's Size Effect Model

So far, we reviewed several size effect models. According to the original Bazant's size effect law, as size decreases the nominal strength approaches the material tensile strength, which is independent of size, and it follows the LEFM size effect law as the size increases. This size effect law might be valid for concrete and other cementitious materials. However, as shown in the previous chapter, cemented sands do not follow his size effect trend. Even though it shows similarities in that the nominal strength for relatively small sizes is close to the tensile strength, the decreasing rate for relatively large size is highly dependent on the particle size. That is because, for concrete, the void is generally filled with paste or cementing agent regardless of the particle size, but cemented sands might not be filled with paste and air void is often left. Since the rate of decrease of the nominal strength is changed with respect to the grain size, Eq (18) is better rewritten as

$$\sigma_N = \frac{Bf_t'}{\left(1+\frac{D}{D_0}\right)^{\alpha}} \quad (19)$$

where, α is the slope of the curve that displays and relates the nominal strength with respect to the geometry size in log-log scale. In order to obtain the slope α at least two data points (nominal strengths with respect to different geometries) for each grain size are required. Unfortunately, for coarse grain size, we obtained data for only the small size of geometry. Therefore it is difficult to say what relationship exists between the slope of the curve and size of grain. Fig. 13 shows α corresponding to the grain size. Since there are only two data points, which are for the fine and the intermediate grain size it can be, for convenience, assumed that the slope changes linearly with respect to the grain size.

With this assumption, let the equation for the linear relationship be described as follows

$$y = ax + b \tag{20}$$

where, y = α, x is the grain size, d_a

If the slope corresponding to a grain size, d_{a1} is α_1 then the eq (20) becomes

$$\alpha_1 = ad_{a1} + b \tag{21}$$

similarly for α_2 corresponding to d_{a2}

$$\alpha_2 = ad_{a2} + b \tag{22}$$

from Eq (21), and Eq (22)

$$a = \frac{\alpha_2 - \alpha_1}{d_{a2} - d_{a1}}$$
$$b = \frac{d_{a2}\alpha_1 - d_{a1}\alpha_2}{d_{a2} - d_{a1}} \tag{23}$$

therefore, Eq (19) can be rewritten as

$$\sigma_N = \frac{Bf_t'}{\left(1 + \frac{D}{D_0}\right)^{ad_a + b}} \tag{24}$$

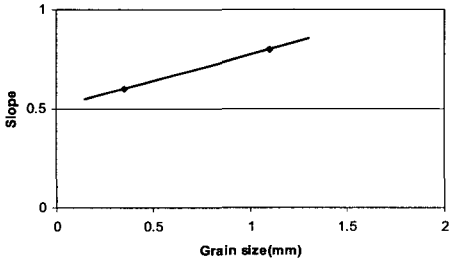

Fig. 13. The slope vs. grain siz

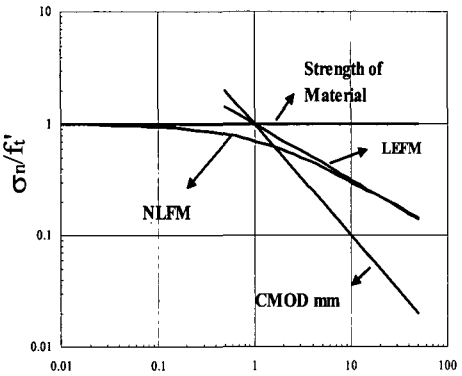

Fig. 14. Size effect with respect to grain size

Fig. 14 presents the nominal strength with respect to the grain size.

6. Conclusion

A series of laboratory experiments were performed to investigate the fracture behavior of cemented sand specimens subjected to shear dominated loading. Three different sizes of specimens and grains were studied, and four-points bending tests were used in the investigation. The effects of grain size and specimen size on fracture characteristics of cemented sand were analyzed. Based on the investigation carried out in this research, we made the following observations and obtained the following results.

- Shear fracture (Mode II) behavior and related fracture properties as well as mixed-mode behavior can be monitored/or obtained by 4-Point beam tests with crack mouth sliding displacement (CMSD) for specimens with the smaller or finer grain size. However, it was difficult to obtain consistent load vs. CMSD response for larger grain sizes.
- This indicates that the inelastic zone in front of the crack tip of the specimens with the coarse sands is relatively small compared to that of the specimens containing finer sands.
- It also indicates that in contrast to the contact bonds existing between the particles in the coarse sands the structure of the specimens with the finer sands is close to the void bond mechanism, where essentially the entire pore space is filled with the cementing agent.
- Cracks propagated not straight up and down, but rather in a sideway or inclined manner. This meant that cracks propagated in mixed-mode.
- LEFM, and CMOD approaches may apply to relatively large structures or specimens, and may not be applicable for small specimen sizes.
- The CMOD approach may be too conservative for geotechnical systems comprising very small grain size materials
- LEFM, and CMOD approaches do not take into account the effect of grain size.

- The modified size effect law shows that it applies to and gives good solutions for a wide range of sizes, and is close to LEFM for small grain size and is becoming conservative as the size increases.
- The modified size effect law takes into account grain size effects far better than any other techniques.

References

1. Alqasabi, A. O. (1998), "Fracture Behavior of Cemented Sand", Ph.D thesis, University of Colorado at Boulder.
2. Bazant, Z. P. (1984), "Size Effect in Blunt Fracture: Concrete, Rock, Metal", *Journal of Engineering Mechanics*, ASCE, 110(4), pp.518-535.
3. Haberfield, C. M., and Johnson, I. W. (1989),"Relationship Between Fracture Toughness and Tensile Strength for Geomaterials", *Proc. of 12th Int. Conf. of Soil Mechanics and Foundations*, Rio DeJaneiro, Brazil, Vol.I, pp.47-52.
4. Iosipescu, N. (1967), "New Accurate Procedure for Single Shear Testing of Metals", *Journal of Materials*, Vol.2, No.3, pp.537-566.
5. Mould, J. C., Jr. (1983), "Stress Induced Anisotropy and the Evaluation of Multi-surface Elasto-plastic Material Model", Ph.D thesis, University of Colorado at Boulder.
6. Rizkallah, J. (1977), "Stress-Strain Behavior of Fissured Stiff Clays", *9th. Int. Conf. on soil Mechanics and Foundation*, Tokyo, Japan, Vol.1, pp.267-270.
7. ASTM Annual Standards (1997), "Standard Test Method for Plane Strain Fracture Toughness of Metallic Materials", ASTM Designation E399-74.
8. Skempton, A.W. (1964), "Long-term Stability of Clay Slopes", *Geotechnique*, Vol.14, pp.77-101.

(received on Mar. 29, 2004, accepted on Aug. 28, 2004)